Zhang, Xiangchao, Jiang, Xiang and Scott, Paul J.

Shape recognition and form error evaluation of quadric surfaces

Shape Recognition and Form Error Evaluation of Quadric Surfaces

Xiangchao Zhang, Xiangqian Jiang and Paul J Scott
Centre for Precision Technologies, University of Huddersfield, Huddersfield, HD1 3DH, UK

1. Introduction

Quadric surfaces are used very extensively in engineering. It has been reported that approximately 85% of manufactured objects can be well-modelled with quadric surfaces [1]. Surface form play an essential role in the characteristics of precision components. To evaluate their form qualities, it is necessary to fit the measured data with an analytical function and obtain the relative deviation.

The most straightforward way to fit data by quadric functions is algebraic fitting. Algebraic fitting's definition of error distances does not coincide with measurement guidelines [3] and the estimated fitting parameters are biased. Here we present an orthogonal distance fitting method applicable for all the quadric surfaces.

2. Shape Recognition

Given a data set $\mathbf{P}$, we obtain a rough guess of its coefficients using the eigen-decomposition method [2].

The general function can be written as,

$$Q(\mathbf{x}) = \mathbf{x}^T\mathbf{K}\mathbf{x} + \begin{bmatrix} G & H & I \end{bmatrix}\mathbf{x} + J = 0$$

with $\mathbf{x} = [x, y, z]^T$.

Perform eigen-decomposition onto the quadric form,

$$\mathbf{K} = \begin{bmatrix} A & D/2 & E/2 \\ D/2 & B & F/2 \\ E/2 & F/2 & C \end{bmatrix} = \mathbf{USU}^T$$

$\mathbf{S}$ is a diagonal matrix with its diagonal entries $\sigma_1 \geq \sigma_2 \geq \sigma_3$
$\mathbf{U}$ is a 3×3 rotation matrix. Assuming $\hat{\mathbf{x}} = \mathbf{U}^T\mathbf{x}$, then

$$Q(\mathbf{x}) = \hat{\mathbf{x}}^T\mathbf{S}\hat{\mathbf{x}} + \begin{bmatrix} G & H & I \end{bmatrix}\mathbf{U}\hat{\mathbf{x}} + J$$
$$= \sigma_1\hat{x}^2 + \sigma_2\hat{y}^2 + \sigma_3\hat{z}^2 + \hat{G}\hat{x} + \hat{H}\hat{y} + \hat{I}\hat{z} + J = 0$$

If $\sigma_1\sigma_2\sigma_3 \neq 0$

$$Q(\mathbf{x}) = \sigma_1(\hat{x} - a_1)^2 + \sigma_2(\hat{y} - a_2)^2 + \sigma_3(\hat{z} - a_3)^2 + a_4 = 0$$

To guarantee the surface representation's uniqueness, the coefficients are scaled by a positive factor.

If $\sigma_3 = 0$,

$$Q(\mathbf{x}) = \sigma_1(\hat{x} - a_1)^2 + \sigma_2(\hat{y} - a_2)^2 + \hat{I}\hat{z} + a_4$$

If $\sigma_2 = 0$, the function can be processed similarly.

If $\sigma_2 = \sigma_3 = 0$,

$$Q(\mathbf{x}) = \sigma_1(\breve{x} - a_1)^2 + \sqrt{\hat{H}^2 + \hat{I}^2}\,\breve{y} + a_4 = 0$$

Table 1. To determine the shapes of quadric surfaces [4]

parameters			shape	Normalisation
$\sigma_1 = \sigma_2$	$\sigma_2 = \sigma_3$		sphere	$a_4 = -1$
	$\sigma_2 > \sigma_3 > 0$		oblate spheroid	
	$\sigma_3 = 0$	$\hat{I} = 0$	Cylinder	$\sigma_1 = 1$
		$\hat{I} \neq 0$	circular paraboloid	
	$\sigma_3 < 0$	$a_4 > 0$	two-sheet circular hyperboloid	$a_4 = 1$
		$a_4 = 0$	Cone	$\sigma_3 = -1$
		$a_4 < 0$	one-sheet circular hyperboloid	$a_4 = -1$
$\sigma_1 > \sigma_2 > 0$	$\sigma_2 = \sigma_3$		prolate spheroid	
	$\sigma_2 > \sigma_3 > 0$		Ellipsoid	
	$\sigma_3 = 0$	$\hat{I} = 0$	elliptic cylinder	
		$\hat{I} \neq 0$	elliptic paraboloid	$\hat{I} = \pm 1$
	$\sigma_3 < 0$	$a_4 > 0$	two-sheet hyperboloid	$a_4 = 1$
		$a_4 = 0$	elliptic cone	$\sigma_3 = -1$
		$a_4 < 0$	one-sheet hyperboloid	$a_4 = -1$
$\sigma_2 = 0$	$\sigma_3 = 0$	$\hat{H} \neq 0$	parabolic cylinder	$\sigma_1 = 1$
		$\hat{H} = 0$	two parallel planes	
	$\sigma_3 < 0$	$\hat{H} \neq 0$	hyperbolic paraboloid	
		$\hat{H} = 0$, $a_4 = 0$	two intersecting planes	
		$\hat{H} = 0$, $a_4 \neq 0$	hyperbolic cylinder	$a_4 = \pm 1$

3. Orthogonal Distance Fitting

In refinement, transformations are always performed onto the data and the quadric surface is represented in a standard implicit form $f(x, y, z) = 0$.

Fitting is carried out in a nested approach $\min_{\mathbf{b}} \sum_{i=1}^{N} \|\mathbf{p}_i - \mathbf{q}_i\|^2$

$\mathbf{q}_i$ is the projection point from $\mathbf{p}_i$ to the surface, and $\mathbf{b}$ is the shape and motion parameters.

The Jacobian matrix at the outer iteration is [5],

$$\mathbf{J}_i = \frac{\partial d_i}{\partial \mathbf{b}} = \frac{\mathrm{sign}\left[\partial f_i / \partial \mathbf{q}_i \cdot (\mathbf{p}_i - \mathbf{q}_i)\right]}{\|\partial f_i / \partial \mathbf{q}_i\|}\left(\frac{\partial f_i}{\partial \mathbf{q}_i}\frac{\partial \mathbf{p}_i}{\partial \mathbf{b}} + \frac{\partial f_i}{\partial \mathbf{b}}\right)$$

The motion and shape parameters are updated using the Levenberg-Marquardt algorithm,

$$(\mathbf{J}^T\mathbf{J} + \lambda\mathbf{I})\delta\mathbf{b} = -\mathbf{J}^T\mathbf{d}$$

4. Numerical Experiments

We compared linear least squares, implicit ODF and specific ODF using a cylinder $x^2 + y^2 = R^2$ (R=1.5 mm) and a cone $\cot\phi\sqrt{x^2 + y^2} = z$ (Φ=45°). The two surfaces were randomly moved to an arbitrary position. The fractal Brownian motion [5] was employed to simulate noise with mean 0 and σ=0.5 μm. The programs were run 150 times.

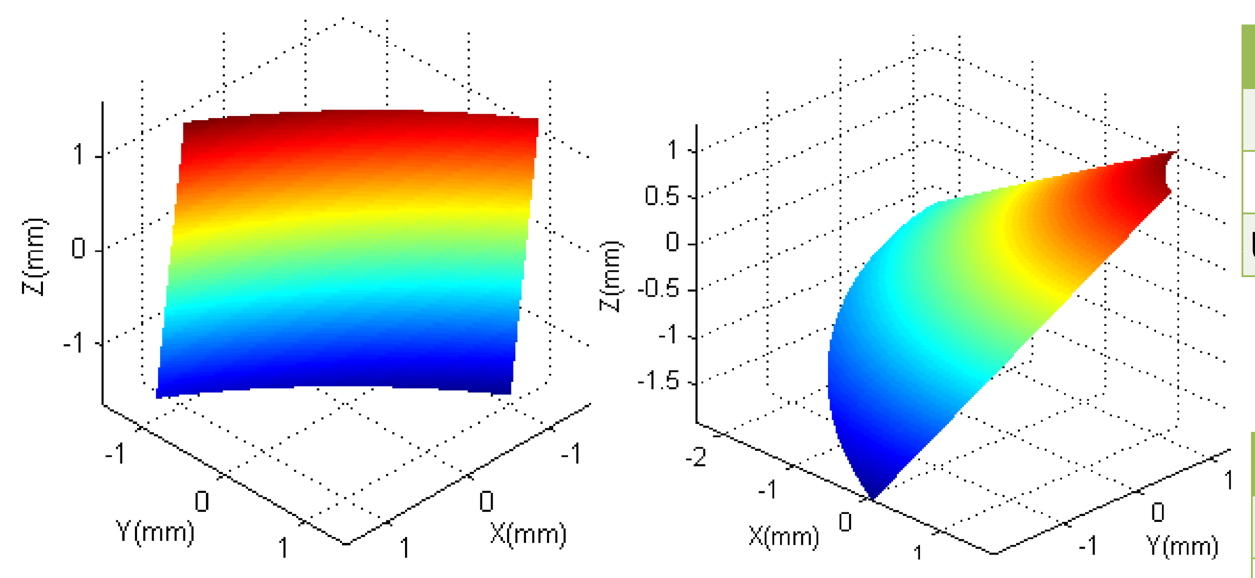

Fig 1. Two standard geometries (a) cylinder and (b) cone

Table 2. Fitting results of cylinder

method	linear		Implicit ODF	Specific ODF
Parameter	σ_1	σ_2	R^2	R
Bias (%)	4.77	-29.75	0.145	-0.045
Uncertainty(%)	502.8	305.3	0.859	0.264

Table 3. Fitting results of cone

method	linear		Implicit ODF	Specific ODF
Parameter	σ_1	σ_2	$\cot^2\Phi$	Φ
Bias (%)	0.941	-1.003	0.163	-0.013
Uncertainty(%)	3.206	3.101	0.295	0.119

Another three quadric surfaces were tested, an ellipsoid $\sigma_1x^2 + \sigma_2y^2 + \sigma_3z^2 = 1$ with σ_1=1, σ_2 =0.5, σ_3 =0.25, a hyperbolic paraboloid $x^2 + \sigma_3z^2 + hy = 0$ with $\sigma^3 = -1$, $h = -2$ mm and a parabolic cylinder $x^2 + hy = 0$ with h =3mm.

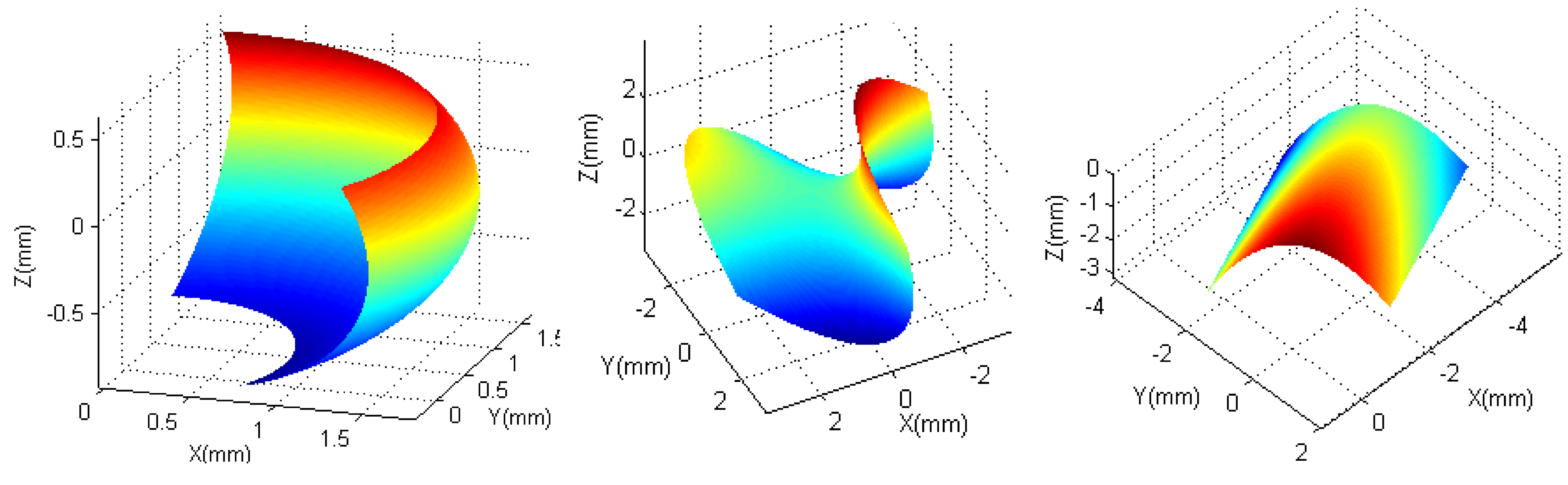

Fig 2. Three quadric surfaces: (a) ellipsoid, (b) hyperbolic paraboloid and (c) parabolic cylinder

The programs were run 150 times and the fitting results of the implicit ODF method are given below,

Table 4. Implicit ODF results of the three quadric surfaces

shape	ellipsoid			hyperbolic paraboloid		parabolic cylinder
Parameter	σ_1	σ_2	σ_3	σ_2	h	h
Bias (%)	-0.012	-0.022	-0.067	0.005	0.002	0.001
Uncertainty(%)	0.188	0.162	0.468	0.041	0.027	0.031

References

[1] PN Chivate and AG Jablokow. Solid-model generation form measured point data. *Comput. Aided Des.* 25(9): 587-600,1993

[2] G Taubin. Estimation of planar curves, surfaces and nonplanar spaces curves defined by implicit equations with applications to edge and range image segmentation. *IEEE Trans. Patt. Anal. Mach. Intell.,* 13(11): 1115-38, 1991

[3] ISO 1101:2004 *Geometrical Product Specifications (GPS)-Geometrical Tolerancing-Tolerances of Form, Orientation, Location and Run-out*

[4] X Zhang. *Free-form Surface Fitting for Precision Coordinate Metrology.* PhD Thesis. University of Huddersfield, UK, 2009

[5] SJ Ahn. *Least Squares Orthogonal Distance Fitting of Curves and Surfaces in Space.* Springer, 2004

[6] BB Mandelbrot and JM Van Ness. Fractional Brownian motions, fractional noises and applications *SIAM Review* 10: 422-37,1968